Pattern formation triggered by rare events: lessons from the spread of rabies

F. JELTSCH, M. S. MÜLLER, V. GRIMM, C. WISSEL AND R. BRANDL

Department of Ecological Modelling, Centre for Environmental Research, UFZ Leipzig-Halle, PO Box 2, D-04301 Leipzig, Germany

SUMMARY

Understanding of large-scale spatial pattern formation is a key to successful management in ecology and epidemiology. Neighbourhood interactions between local units are known to contribute to large-scale patterns, but how much do they contribute and what is the role of regional interactions caused by long-distance processes? How much long-distance dispersal do we need to explain the patterns that we observe in nature? There seems to be no way to answer these questions empirically. Therefore, we present a modelling approach that is a combination of a grid-based model describing local interactions and an individual-based model describing dispersal. Applying our approach to the spread of rabies, we show that in addition to local rabies dynamics, one long-distance infection per 14000 km^2 per year is sufficient to reproduce the wave-like spread of this disease. We conclude that even rare ecological events that couple local dynamics on a regional scale may have profound impacts on large-scale patterns and, in turn, dynamics. Furthermore, the following results emerge: (i) Both neighbourhood infection and long-distance infection are needed to generate the wave-like dispersal pattern of rabies; (ii) randomly walking rabid foxes are not sufficient to generate the wave pattern; and (iii) on a scale of less than 100 km × 100 km, temporal oscillations emerge that are independent from long-distance dispersal.

1. INTRODUCTION

Dispersal is a key process in spatially structured populations. Recent models show that interactions between local populations by dispersal may generate complex spatial patterns (Hengeveld 1989). Previous approaches of spatio-temporal modelling aggregate the dispersal process in the diffusion coefficient either in continous or discretized space (Hengeveld 1989). This diffusion approach was successful in describing the spread of species on a biogeographical scale (Skellam 1951; Lubina & Levin 1988; Okubo *et al*. 1989), but ignores the particular way in which individuals disperse through a landscape. Although dispersing individuals may react in a complex manner to local ecological situations (Lima & Zollner 1996; Schippers *et al*. 1996) and rare long-distance dispersal events may be important in nature (Jeltsch *et al*. 1996), the modelling methods that summarize dispersal in a diffusion coefficient allow no insights into the mechanisms of spatial pattern formation or the importance of rare events.

Individual-based modelling (DeAngelis & Gross 1992; Uchmański & Grimm 1996) seems to offer an appropriate alternative to analysing the mechanisms of pattern formation. But modelling the entire life history of each individual in time and space generates an enormous complexity of information that necessarily limits the interpretation and application of model results. In the spread of rabies, for example, the spatial scale of individual-based models is restricted by the number of individuals and the amount of data that can be processed. A promising approach, however, in modelling spatio-temporal phenomena is the combination of grid-based models and individual-based models of dispersal. This spatially discrete approach provides a wide range of choices for aggregating the description of within-grid cell dynamics. In the extreme, one may aggregate the dynamics into a small number of discrete states (cellular automata; compare Wolfram (1986) and Jeltsch & Wissel (1994)). This simplification of the local dynamics allows a detailed analysis of the large-scale patterns triggered by different dispersal strategies. To demonstrate the power of this approach we model the spread of rabies, as the variety of different rabies models that have appeared in the literature (Preston 1973; Anderson *et al*. 1981; Källén *et al*. 1985; Murray *et al*. 1986; Smith & Harris 1991; Barlow 1995; White *et al*. 1995) over recent years allows us to fully evaluate the potential of the suggested approach.

2. BIOLOGICAL BACKGROUND

Rabies is a virus disease of the central nervous system transmitted by the injection of infected saliva. In central Europe the principal wildlife reservoir for the disease is the red fox (*Vulpes vulpes*) (Wandeler *et al*. 1974; Macdonald & Voigt 1985). Once infected, foxes incubate the disease for an average of three weeks. They

then become infective and shed virus for about one week. Symptoms appear, after which the fox will survive for a maximum of 4 d: high, irregular mobility, paralysis, or a docile, friendly approach to normally frightening stimuli (Wandeler *et al.* 1974; Macdonald & Voigt 1985).

The present European epidemic of rabies originated in Poland about 50 years ago and spread at an annual rate of 20–60 km (Toma & Andral 1977; Steck & Wandeler 1980). The highest incidence of fox rabies is recorded in the front wave, with about 25–50% of the total fox population being killed by the disease. The reduction of fox density by rabies disrupts the chain of infection. However, after the recovery of fox density above a critical level, new waves may start from scattered foci of rabies behind the initial front wave. The reappearance of rabies behind the front causes a damped, wave-like spreading pattern with peaks recurring at 4–5 years. Seasonally, most infections are recorded during late winter. There is a similar peak in the monthly velocity of the front line, with values around 5 km during summer and 15–20 km during winter (Toma & Andral 1977; Steck & Wandeler 1980).

There is a lot of local variation of the epizootic pattern with local environmental conditions, fox density and the associated behavioural variation between fox populations. Hence the study of rabies transmission is linked to the study of its vectoral behaviour. Foxes tend to be restricted to discrete home ranges. In Central Europe, home range size is about 4 km², but this may differ considerably between areas (range 2.5–16 km²) (Harris & Trewhella 1988; Trewhella *et al.* 1988). Each home range is typically occupied by a family group of one adult male and one or two adult females. In spring, one female produces four or five cubs, with a sex ratio of 1:1. Juveniles leave their home ranges between October and March (Harris & Trewhella 1988), with a dispersal peak during October and November (Steck & Wandeler 1980), and disperse into new terrain. Dispersal distances are influenced by the local environment, sex and population density. In Central Europe, mean dispersal distance is between 5 and 10 km with maximum values above 20 km, sometimes above 100 km (Jensen 1973; Steck & Wandeler 1980). Dispersers leave their home ranges in a more or less straight line with random direction (Storm & Montgomery 1975; Storm *et al.* 1976). Encounters between individuals of adjacent groups are uncommon, almost always agressive and occur significantly more often in winter. The highest incidence of bite wounds occurred in winter and spring, coincident with the mating and dispersal seasons (White & Harris 1994).

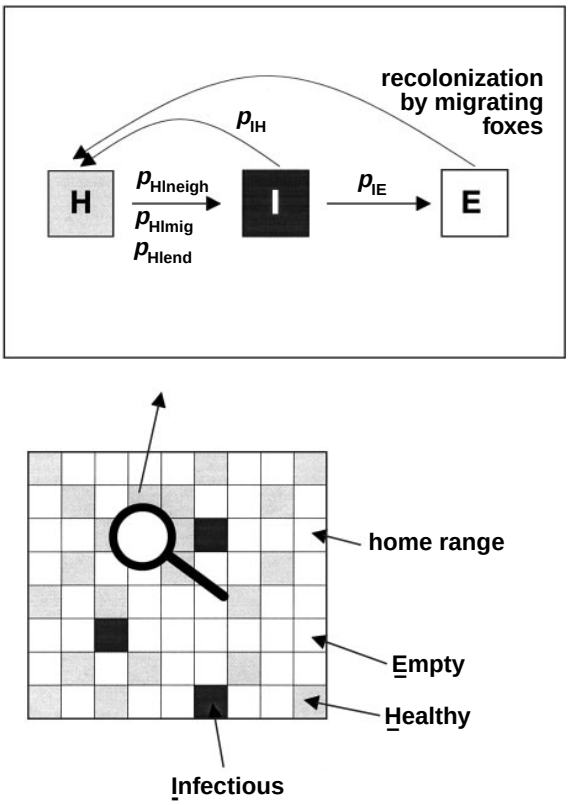

Figure 1. Schematic model description. An idealized homogeneous area is subdivided into a grid of cells representing the fox home ranges. The size of the modelled area was varied systematically up to a maximum of 2000 × 2000 home ranges. The description of the local dynamics within a fox home range is aggregated into discrete states on a temporal basis of two months. The transitions between these states occur with certain probabilities either throughout the year (transition from state I to state E or state H, transition from state H to state I caused by neighbourhood infection), or only during the dispersal phase (transition from state E to state H, transition from state H to state I caused by migrating infectious foxes). The parameters, their meanings and a standard set of values are given in table 1.

3. THE MODEL

The cells of the grid in our model represent fox home ranges of an average size in an idealized homogenous area. The interaction between family groups living in the home ranges occurs through two processes acting on different scales: neighbourhood infection and dispersal (figure 1). Within-home range dynamics is modelled by discrete states (compare Jeltsch & Wissel (1994) and Jeltsch *et al.* (1996)) describing the fate of healthy or infected fox family groups (figure 1). We distinguish three discrete states on a temporal basis of two months (one timestep), i.e. 'H'—healthy fox population, 'I'—infectious fox population, 'E'—empty home range. The states of all cells are updated simultaneously. The transitions between these states occur with certain probabilities, e.g. p_{IE} is the probability of a transition from state I to state E within two months. The transition from state E to state H, the recolonization, occurs during the dispersal phase. The 'infection' of a home range, i.e. the transition from H to I, is modelled by three differing probabilities corresponding to three different infection modes. First, $p_{HIneigh}$ describes the probability that a home range in state H is infected in a timestep by a neighbouring home range in state I. This infection mode may occur throughout the year. Second, p_{HImig} is the probability that a home range in state H is infected by a migrating fox (originating from a home range in state I) passing

Table 1. *Parameters of the model*

parameter	meaning	standard value
p_{HIneigh}	probability of home range transition from state H to state I within one time-step; 'infection' by neighbouring home range	40 %
p_{HImig}	probability of home range infection by a migrating infected fox passing through	10 %
p_{HIend}	probability of home range infection by a migrating infected fox at the end of migration	70 %
p_{IH}	probability of home range transition from state I to state H	15 %
p_{IE}	probability of home range transition from state I to state E	80 %
maxdist	maximal dispersal distance of migrating foxes	60 home ranges
mig	number of offspring leaving the birth home range	4
p_{end}	probability of ending the dispersal of a migrating fox after passing through *step* home ranges	$0.2+0.8\times step/maxdist$ (empty home range) $0.05+0.35\times step/maxdist$ (non-empty home range)
p_{left}	probability of the next inter-home range dispersal step of a migrating fox being to the left of the main direction	25 %
p_{main}	probability of the next inter-home-range dispersal step being in the main direction	50 %
p_{right}	probability of the next inter-home-range dispersal step being to the right of the main direction	25 %

through the home range, or third, p_{HIend} is the probability of being infected by a migrating fox ending its migration in the home range either by settling down or by dying. The last two modes only occur during the dispersal phase if a migrating fox enters the home range in state H. During the time-step of dispersal, infection by migrating foxes and neighbourhood infection occur consecutively. Dispersal is modelled by an individual-based approach (Smith & Harris 1991; Dunning *et al*. 1995). Individual subadult foxes are modelled to leave their birth home ranges during the migration phase and to colonize empty home ranges. If they are infective they may thus spread the disease. The migration behaviour of healthy and infected foxes is not distinguished, but infected foxes are not able to colonize an empty home range. The corresponding probability is, in this case, interpreted as the probability of dying in the home range. The dispersal phase is modelled to occur completely within one time-step of two months: a variable number of young foxes (parameter *mig*, ignoring differences of males and females) leave their birth home range, each of them randomly choosing a main direction of migration. In each migration step (which is independent from the two-month time-step of the model) each individual fox migrates from the home range of its actual position to a neighbouring home range. With a probability p_{main} it moves to a home range in the main direction. The two adjacent home ranges are chosen with a smaller probability (p_{left}, p_{right}), all three probabilities add up to 100 %. This simple approach leads to a more or less straight dispersal direction similar to those observed in nature (Trewhella *et al*. 1988), with the probability p_{end} that the fox remains in the home range of its current position. If a fox originating from a home range in state H ends its migration in an empty home range (state E) this probability includes a successful colonization. If, in contrast, the home range is already occupied (state H or state I) it is not distinguished whether the fox is integrated into the social group or whether it dies. In accordance with empirical findings, p_{end} is modelled to increase with the migrated distance (Trewhella *et al*. 1988). For simplicity a linear increase up to a maximal dispersal distance, *maxdist*, is chosen. The resulting dispersal distance of a migrating fox depends on the product of the probabilities to continue the migration ($1-p_{\mathrm{end}}$) of all home ranges the fox passed through and the probability, p_{end}, of its final position. Hence, the dispersal distance distribution is realistically skewed, with most animals moving relatively short distances and few animals moving far. The probability of remaining in an empty home range (p_{end}) is modelled with a higher slope and intercept than in an occupied home range (see table 1). The migration module outlined above is only one possible example of processing the available information about fox dispersal. However, the chosen individual-based approach is able to include a variety of behavioural characteristics (see below).

The parameters, their meanings, and a standard set of values are given in table 1. Because most model parameters represent highly aggregated biological information, direct empirical evidence for single parameter values is difficult to obtain. Thus, the parameters were systematically varied over wide ranges; standard values were chosen in order to represent the empirical information available.

The model was implemented in C++, and simulations were run on both PC and IBM RS/6000 workstations.

4. RESULTS AND DISCUSSION

Figure 2*a* shows a typical spatial pattern and its one-dimensional projection. The model reproduces the wave-like pattern of the spread of rabies for a wide range of parameters. The mean velocity of the first wave (v) is 27.13 home ranges per year and the mean

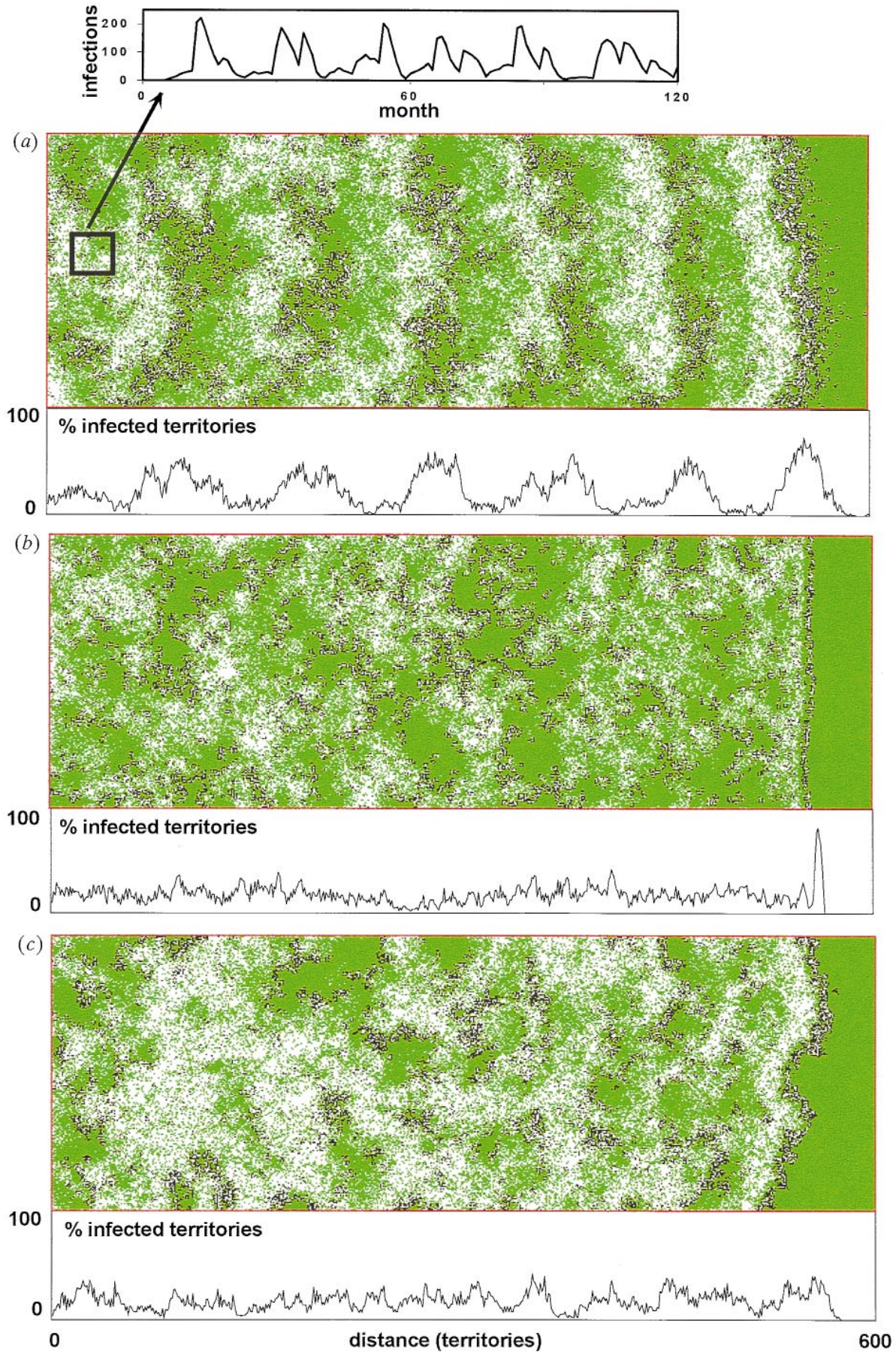

Figure 2. Snapshots of the large-scale distribution pattern in a region of 600 × 300 home ranges and a one-dimensional projection of this pattern, showing the number of infected home ranges in a three home range-wide strip at certain distances to the left border of the region: (*a*) after 120 time-steps; (*b*) after 570 time-steps; (*c*) after 216 time-steps; note

distance (*dx*) between the front and second wave is 93.15 home ranges, which are both in the range of empirically observed values (Steck & Wandeler 1980; Källén *et al.* 1985; Murray *et al.* 1986). Both of these dispersal pattern characteristics are mainly determined by the maximal dispersal distance of migrating young foxes (*maxdist*, figure 4). But how do the two different modes of coupling, neighbourhood infection, and dispersal contribute to this pattern? Suppressing the dispersal of infected young foxes, while leaving the rest of the model unchanged, leads to the disappearance of the wave pattern (figure 2*b*). Dispersal of subadults is thus the crucial mechanism that generates the large-scale pattern. On a more local spatial scale of approximately 40×40 home ranges, however, neighbourhood infection still induces a spatial autocorrelation (figure 2).

It has been hypothesized that randomly walking rabid foxes are the main source of the wave pattern (Murray *et al.* 1986). To test this hypothesis, we use a further modification of the model, where dispersal is limited to randomly walking rabid foxes. The random walk module is designed to produce an upper limit of empirically observed walking distances of foxes (Jensen 1973; Anderson *et al.* 1981): during each time-step from each infected home range a rabid fox starts a random walk with a probability of 0.11. The fox infects home ranges on its way with a probability of 0.5, and will travel a maximum distance of 30 home ranges. The probability that the fox dies on its way increases linearly with time, $p_{\mathrm{mort}} = 0.01 + steps \times (0.01/50)$, where *steps* is the number of home ranges the fox passed through during that particular random walk. Results show that no marked wave structure emerges behind the infection front in this case either (figure 2*c*). This and other variants of the random walk cause no long-distance correlation of the disease because the area covered by the movement of rabid foxes is more localized than for the original, more or less linear dispersal mechanism.

Irrespective of the dispersal mechanism there are pronounced local temporal oscillations in the occurence of rabies over areas up to a size of about 40×40 home ranges (figure 2*a*). These temporal oscillations occur in all variants of the model investigated and are thus not linked to the occurrence of the large-scale wave pattern. They reflect a local correlation caused by neighbourhood infection between home ranges. These oscillations have been observed in different parts of Europe (Wandeler *et al.* 1974; Macdonald & Voigt 1985). Despite the extreme aggregation of information in the state-and-transition description of the local dynamics (figure 1), our model is able to reproduce the local dynamics of the epidemics realistically (figure 2).

In contrast to other models that reproduce the wave-like pattern (Preston 1973; Anderson *et al.* 1981; Källén *et al.* 1985; Murray *et al.* 1986; Smith & Harris 1991), we have demonstrated the generation of the pattern as an interplay of neighbourhood infection and long-distance dispersal (figure 3).

During the first five time-steps, the disease spreads slowly by neighbourhood infection, followed by a leap caused by the dispersal of young infected foxes (time-step 6). Behind the front wave, empty home ranges are recolonized by dispersing foxes from remnant healthy home ranges in that region itself and from the region in front of the wave (time-step 12). This allows for a small backwards propagating wave of the epidemic to build up (time-step 14). Although fading out (time-step 17), this wave leaves scattered remnants of the disease (time-step 18). During dispersal (time-steps 18 and 24) empty home ranges are recolonized in the area between front wave and backward wave. This causes a situation similar to the intial conditions: a healthy region almost free of rabies and a strip of infected home ranges to the left of this region (time-step 24). Consequently, a second wave builds up that follows the front wave. The same mechanism produces further waves.

The foci of infection caused by infected foxes travelling long distances play a decisive role in the process of wave generation. The foci can be traced for several years (see the history of the marked focus in figure 3). Thus, rabies progresses as foci of disease incidence that propagate seperately and independently, causing a complex structure of the wave front as emphasized in empirical studies analysing rabies records (Sayers *et al.* 1985; Hengeveld 1989).

The model results proved to be very robust towards variations of the parameters within wide ranges (figure 4). However, for certain parameters the most likely 'real' values may lie somewhere towards the left of the *x*-axis where there is considerable variation in the results. Variations in the probability of neighbouring infection p_{HIneigh} show that once a certain threshold of approximately 20% is reached the wave-like pattern occurs (row 1, column 2 of figure 4). Thus a certain amount of neighbourhood infection is necessary to generate the pattern. But, as has been shown in figure 3*b*, this alone is not sufficient to produce the wave pattern. In addition, at least one fox per infected home range has to disperse over large distances (row 2, column 2 of figure 4). An increase in the maximum distance covered by dispersing subadult foxes leads to

that each time-step is two months). Healthy home ranges are green, infected home ranges are black, and empty home ranges white. (*a*) Pattern produced by the full model (see figure 1; for parameters see table1). The waves become increasingly frayed with increasing distance from the wave front, but can still be clearly identified in the projection throughout the entire region. The time series of the occurrence of rabies in the 30×30 home ranges sample square (indicated in figure 2*a*) shows the recurrent temporal fluctuations of infected home ranges on a local scale. Similar local fluctuations occur in all tested model versions. (*b*) Pattern produced by the model without dispersal of infected foxes. The velocity of the spread of rabies is much lower than in the full model (*a*). The distribution is patchy, but no waves occur. (*c*) Pattern produced by the model without dispersal of infected foxes in the migration period, but rabid foxes show a high irregular mobility during each time-step (random walk). Again no wave pattern emerges.

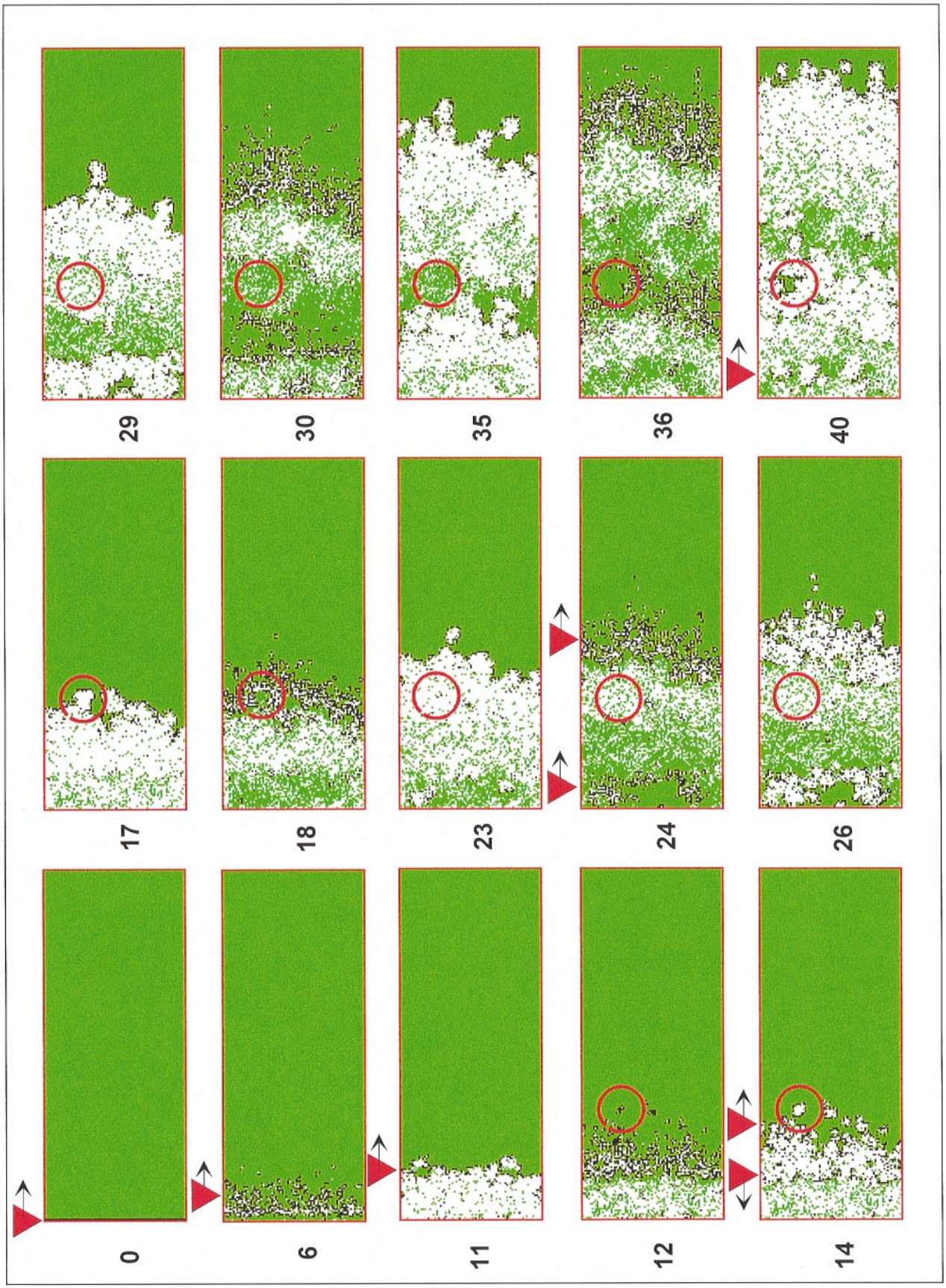

Figure 3. The spread of rabies into a region of 200 × 80 home ranges. Initially, a one home range-wide strip on the left is infected (step 0). Time-steps 6, 12, 18, etc., are the periods of long-distance dispersal. Healthy home ranges are green, infected home ranges are black, and empty home ranges are white. Triangles at the frame indicate wave fronts referred to in the text. The red circle highlights the fate of one focus of infection. For further details see figure 2*a* and table 1.

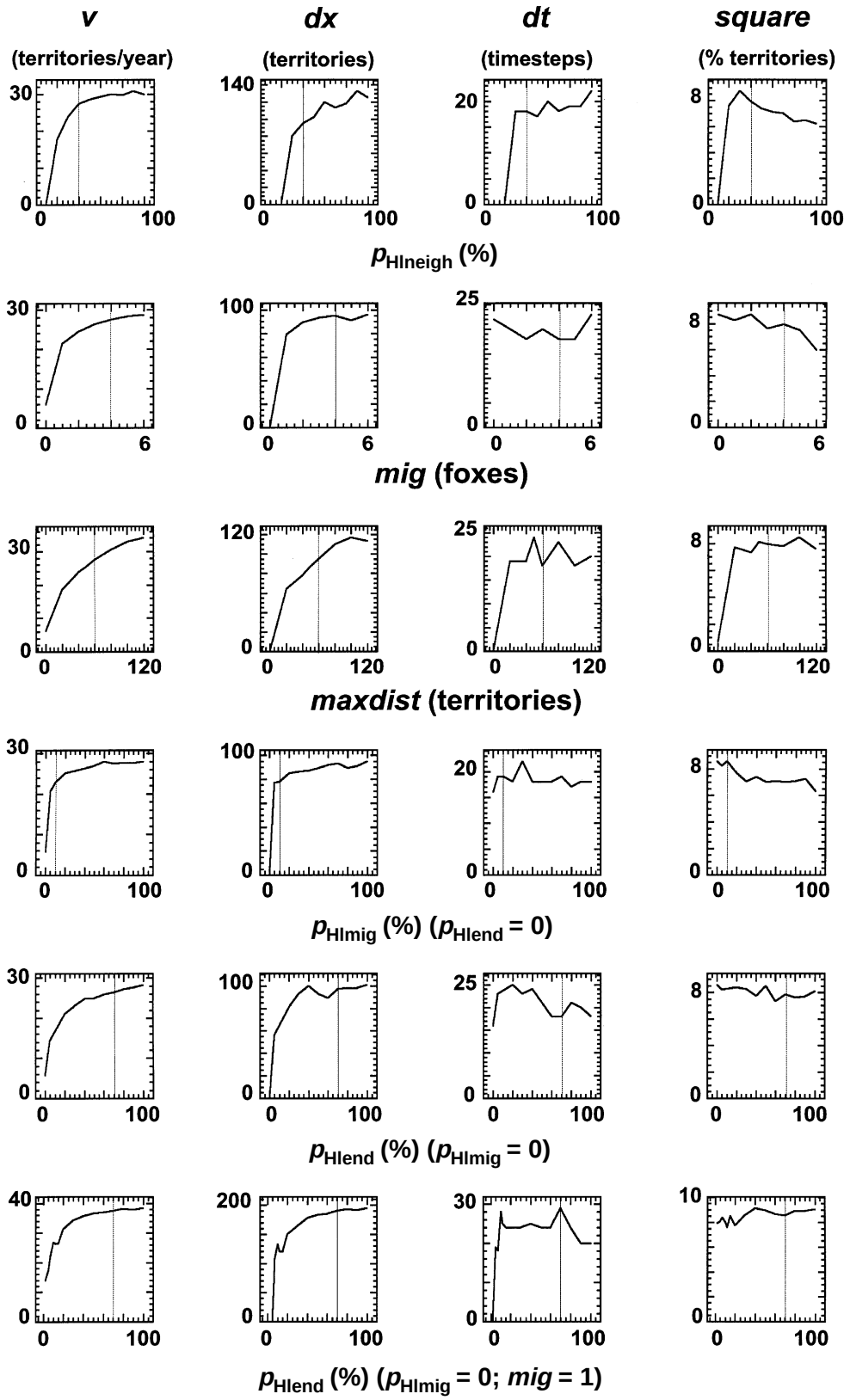

Figure 4. Sensitivity analyses of the model. Each row stands for a certain model parameter which is varied (see table 1), and each column for a certain measure that quantifies the distribution pattern. v: velocity of the front wave; dx: distance between the front wave and the second wave (if $dx > 0$ we have at least two distinct propagating waves); dt: time between the first and second maximum of the time series from figure 2*a*; *square*: mean percentage of infected home ranges in the sample square shown in figure 2*a*. Sampling starts at the first occurrence of rabies in the sample square. The standard value of each varied parameter is indicated by a line. Deviations from the set of standard parameters given in table 1 (rows 4, 5 and 6) are given in parentheses. These model modifications were implemented to investigate the relative importance of the two infection modes: neighbourhood infection and infection by long-distance dispersal. In contrast to the standard model, the dispersal distance of migrating foxes in row 6 was fixed at 40 home ranges to test the influence of long-distance migrating foxes only.

an increased velocity of the first wave front (v) and to larger distances between the peaks (dx) (row 3, figure 4) but does not change the general wave-like structure. Rows 4 and 5 show the situation where infection either occurs during migration ($p_{\mathrm{HIend}} = 0$; row 4) or at the end of it ($p_{\mathrm{HImig}} = 0$; row 6). Both modes generate a wave pattern, even at low infection probabilities. This result suggests that the generation of the large-scale pattern requires only a few events of disease transmission.

To pin-point the meaning of rare long-distance infection events we reduced the number of dispersing infected foxes to one fox per infected home range. In addition, the dispersal distance was fixed at a constant 40 home ranges. Thus only long-range dispersing infected foxes are modelled (row 6, figure 4). The parameter p_{HIend} is the probability that a fox infects the home range at the the end of its migration. Even extremely low infection probabilities generate the wave pattern. Counting the number of infections (as measured by transitions of the home range from state H to state I) shows that the number of infections caused by migrating foxes in this scenario is only 2% of the number of infections caused by migrating foxes in the full model, as described in figure 1 and table 1. A mean number of one long-distance infection per 14 000 km^2 per year is sufficient to generate the typical large-scale spread and pattern of rabies. (In the modified model the migrating foxes caused, on average, 118 infections per year in the total modelled area of 1.6×10^6 km^2 whereas in the full model, as described in figure 1 and table 1, 6026 infections by migrating foxes occurred per year in that area.)

Diffusion models proved to be successful in describing the general wave-like structure of the spread of rabies on large spatial scales, whereas individual-based models, including detailed fox behaviour, allowed small-scale descriptions (Preston 1973; Anderson *et al.* 1981; Källén *et al.* 1985; Murray *et al.* 1986; Smith & Harris 1991). Both approaches are opposite extremes in aggregating biological information. The presented approach of incorporating an individual-based into a grid-based model offers the possibility of choosing any point on the scale of aggregation created by those extremes. As pointed out in the Introduction, an understanding of the coupling between the small- and large-scale distribution of species requires a thorough analysis of the dispersal process. The importance of contacts between neighbouring groups in the process of pattern formation is emphasized by White *et al.* (1995). We show that rare long-distance infections generate foci of rabies that persist for long periods, and thus act as a local record of former spatial structures. In combination with the synergistic effects of the local neighbourhood infection, a complex spatially and temporally correlated structure emerges. Thus, rare events are responsible for the velocity of the epizootic (Goldwasser *et al.* 1994) and are essential in the formation of the spatial pattern. Even though rare events are difficult to record during empirical studies, we show that it is possible to retrieve their importance by using the overall large-scale pattern as an ecological fingerprint (Grimm *et al.* 1996).

REFERENCES

Anderson, R. M., Jackson, H. C., May, R. M. & Smith, A. M. 1981 Population dynamics of fox rabies in Europe. *Nature, Lond.* **289**, 765–771.

Barlow, N. D. 1995 Critical evaluation of wildlife disease models. In *Ecology of infectious diseases in natural populations* (eds. B. T. Grenfell & A. P. Dobson). Cambridge University Press.

DeAngelis, D. L. & Gross, L. J. (eds) 1992 *Individual-based models and approaches in ecology: populations, communities and ecosystems*. New York and London: Chapman & Hall.

Dunning, J. B., Stewart, D. J., Danielson, B. J. N. R., Noon, B. R., Root, T. L., Lamberson, R. H. & Stevens, E. E. 1995 Spatially explicit population models: current forms and future uses. *Ecol. Appl.* **5**, 3–11.

Goldwasser, L., Cook, J. & Silverman, E. D. 1994 The effects of variability on metapopulation dynamics and rates of invasion. *Ecology* **75**, 40–47.

Grimm, V., Frank, K., Jeltsch, F., Brandl, R., Uchmański, J. & Wissel, C. 1996 Pattern-oriented modelling in population ecology. *Sci. Total. Environ.* **183**, 151–166.

Harris, S. & Trewhella, W. J. 1988 An analysis of some of the factors affecting dispersal in an urban fox (*Vulpes vulpes*) population. *J. Appl. Ecol.* **25**, 409–422.

Hengeveld, R. 1989 *Dynamics of biological invasions*. London, New York: Chapman & Hall.

Jeltsch, F., Milton, S. J., Dean, W. R. J. & van Rooyen, N. 1996 Tree spacing and coexistence in semiarid savannas. *J. Ecol.* **84**, 583–595.

Jeltsch, F. & Wissel, C. 1994 Modelling dieback phenomena in natural forests. *Ecol. Model.* **75/76**, 111–121.

Jensen, B. 1973 Movements of the red fox (*Vulpes vulpes*) in Denmark investigated by marking and recovery. *Dan. Rev. Game Biol.* **8**, 3–20.

Källén, A., Arcuri, P. & Murray, J. D. 1985 A simple model for the spatial spread and control of rabies. *J. Theor. Biol.* **116**, 377–393.

Lima, S. L. & Zollner, P. A. 1996 Towards a behavioural ecology of ecological landscapes. *Trends Ecol. Evol.* **11**, 131–135.

Lubina, J. A. & Levin, S. A. 1988 The spread of a reinvading species: range expansion in the California sea otter. *Am. Nat.* **131**, 526–543.

MacDonald, D. W. & Voigt, D. R. 1985 The biological basis of rabies models. In *Population dynamics of rabies in wildlife* (ed. P. J. Bacon), pp. 71–108. London: Academic Press.

Murray, J. D., Stanley, E. A. & Brown, D. L. 1986 On the spatial spread of rabies among foxes. *Proc. R. Soc. Lond.* B **229**, 111–150.

Okubo, A., Murray, J. & Williamson, M. 1989 On the spatial spread of grey squirrels in Britain. *Proc. R. Soc. Lond.* B **238**, 113–125.

Preston, E. M. 1973 Computer simulated dynamics of a rabies-controlled fox population. *J. Wildlife. Manage.* **37**, 501–512.

Sayers, B. McA., Ross, J. A. & Saengcharoenrat, P. 1985 Pattern analysis of the case occurrences of fox rabies in Europe. In *Population dynamics of rabies in wildlife* (ed. P. J. Bacon), pp. 235–254. London: Academic Press.

Schippers, P., Verboom, J., Knaapen, J. P. & van Apeldoorn, R. C. 1996 Dispersal and habitat connectivity in complex heterogeneous landscapes: an analysis with a GIS-based random walk model. *Ecography* **19**, 97–106.

Skellam, J. G. 1951 Random dispersal in theoretical populations. *Biometrika* **38**, 196–218.

Smith, G. C. & Harris, S. 1991 Rabies in urban foxes (*Vulpes vulpes*) in Britain: the use of a spatial stochastic simulation model to examine the pattern of spread and evaluate the efficacy of different control regimes. *Phil. Trans. R. Soc. Lond.* B **334**, 459–479.

Steck, F. & Wandeler, A. 1980 The epidemiology of fox rabies in Europe. *Epidemiol. Rev.* **2**, 72–96.

Storm, G. L., Andrews, R. D., Phillips, R. L., Bishop, R. A., Sineff, D. B. & Tester, J. R. 1976 Morphology, reproduction, dispersal and mortality of mid-western fox populations. *Wildlife Monogr.* **49**, 1–82.

Storm, G. L. & Montgomery, G. G. 1975 Dispersal and social contact among red foxes: results from telemetry and computer simulation. In *The wild canids* (ed. M. W. Fox), pp. 237–246. New York: Van Nostrand Reinhold Co.

Toma, B. & Andral, L. 1977 Epidemiology of fox rabies. *Adv. Virus Res.* **21**, 1–36.

Trewhella, W. J., Harris, S. & McAllister, F. E. 1988 Dispersal distance, home range size and population density in the red fox (*Vulpes vulpes*): a qualitative analysis. *J. Appl. Ecol.* **25**, 423–434.

Uchmański, J. & Grimm, V. 1996 Individual-based modelling in ecology: what makes the difference? *Trends Ecol. Evol.* **11**, 437–441.

Wandeler, A., Wachendörfer, G., Förster, U., Krekel, H., Schale, W., Müller, J. & Steck, F. 1974 Rabies in wild carnivores in central Europe. 1. Epidemiological studies. *Zbl. Vet. Med.* B **21**, 735–756.

White, P. C. L. & Harris, S. 1994 Encounters between red foxes (*Vulpes vulpes*): implications for territory maintenance, social cohesion and dispersal. *J. Anim. Ecol.* **63**, 315–327.

White, P. C. L., Harris, S. & Smith, G. C. 1995 Fox contact behaviour and rabies spread: a model for the estimation of contact probabilities between urban foxes at different population densities and its implication for rabies control in Britain. *J. Appl. Ecol.* **32**, 693–706.

Wolfram, S. 1986 *Theory and application of cellular automata*. Singapore: World Science Publishers.

Received 9 December 1996; accepted 20 December 1996

As this paper exceeds the maximum length normally considered for publication in *Proceedings* B, the authors have agreed to make a contribution towards production costs.